



The de-stripping of the VIMS-V images and the observations of HCN limb emission in the Titan atmosphere at $3 \mu\text{m}$

A. Adriani¹, M. L. Moriconi², G. Filacchione³, F. Tosi¹, A. Coradini¹, R. H. Brown⁴,
and the Cassini-VIMS team

¹ Istituto Nazionale di Astrofisica – Istituto di Fisica dello Spazio Interplanetario, via del Fosso del Cavaliere 100, I-00133, Rome, Italy

² Consiglio Nazionale delle Ricerche – Istituto di Scienze dell’Atmosfera e Clima, via del Fosso del Cavaliere 100, I-00133, Rome, Italy

³ Istituto Nazionale di Astrofisica – Istituto di Astrofisica Spaziale e Fisica Cosmica, via del Fosso del Cavaliere 100, I-00133, Rome, Italy

⁴ Department of Planetary Sciences, and Lunar and Planetary Laboratory, University of Arizona, 1629 E. University Boulevard, Tucson, AZ 85721, USA

Abstract. In this paper two different tools for the analysis of VIMS hyperspectral images will be presented. A statistical methodology has been realized to correct the striped appearance of the VIMS-V images. This destripping procedure applies to each pixel of the images in the visible range and can be used both for the raw and calibrated data. Respect to their original values, the 60% of the destripped pixels fall in a 1% range, the 93% fall in a 2% range and finally all the pixels fall in a 3% range. A second tool regarded the detection of minor species at different heights, as suggested by the check of the VIMS-IR images for the Titan’s limb at high phase angles. The spectral examination of the image pixels at the limb emphasized three features at 3.03 , 3.33 e $4.78 \mu\text{m}$, assigned by the literature to HCN and CH_4 fluorescence and to a probable CO thermal emission respectively. An estimation of the maximum concentration level for the three species has been done by combining a simple algorithm and easy geometrical calculations.

Key words. Titan: atmosphere – Image processing

1. Introduction

The remote sensing measurements in the shortwave range are commonly used to analyze the aerosol properties, by radiative transfer considerations. This information, together with the atmospheric absorbing properties derived from the mid and long wave spectral measurements, is used for the at-sensor radiance analysis, by allowing for the separation and the weighting of the ground and the atmosphere contributions. The Cassini VIMS-V channel operates in the wavelength range $0.3 - 1.05 \mu\text{m}$, with a (nominal) spectral resolution of 7.3 nm and a (nominal) spatial

Send offprint requests to: A. Adriani

resolution of 0.5 mrad. The VIMS-V images of Titan, unlike the VIMS-IR images, present frequently a striped appearance, not always removed by the standard calibration procedure. For this reason a statistical methodology has been thought to correct this particular aspect of the VIMS-V images. This procedure has been realized for the qube V1514302573, band 66 (827.21 nm), got as a case study, and it was successfully tested on other VIMS-V images. The retrieval of atmospheric compositions and molar fraction profiles need generally some competences about photochemical models, availability of spectrophotometer measurements and a good knowledge of molecular spectroscopy. A simple tool to estimate the maximum concentration levels for some minor components in the Titan atmosphere has been set up on the base of the differential absorption method, applied to a number of limb spectra, collected from the surface to the TOA (Top of Atmosphere), and calculating the atmospheric layer thickness on the base of the image spatial resolution, of the spacecraft distance from the Titan surface and of the effective IFOV value for the IR channel.

2. The methodology for VIMS-V image correction

The correction procedure starts from the ascertainment that the inhomogeneities in the VIMS-V images are organized by samples (vertical lines or image columns), as it is clearly shown in the image in Fig. 1 ¹

$$\bar{S}_j = \frac{1}{n} \sum_i S_{ij} \quad (1)$$

Then the methodology for inhomogeneities or stripes removing (hereafter named destriping procedure) is based on the fact that such a noise is a characteristic of the image samples, namely it is a noise electronically added during the CCD read out process in the same amount to all the pixels constituting a single image sample. As a global effect, a modulation along the image lines is eventually introduced. Following this criterion, the mean line signal intensity can be computed applying the expression: for $i=1, n$ and $j=1, m$ where n is the number of lines and m is the number of samples for each image. This permitted the construction of a function, \bar{S}_j , which emphasize the stripe noise characteristics. The successive step is the filtering out of the high frequency noise on \bar{S}_j (black curve in Fig. 2) by applying an "edge truncated smoothing algorithm" from the IDL library, in order to create the new function \bar{S}_j^s (blue curve in Fig. 2).

The $\bar{S}_j - \bar{S}_j^s$ residual represents the amount of stripe noise to be removed from all the pixels of the corresponding j -sample. The result of the residual removal is shown in Fig. 3. The departure of the corrected (or destriped) value of the intensity of each image pixel, obtained by the application of the destriping procedure, from its original value is reported in the histogram of figure 4. The histogram gives the statistics of the procedure applied to the band 66 image (827.21 nm), got from the qube V1514302573. The histogram shows that about 60% of the pixels falls under a correction lower than $\pm 1\%$ of its original value, about the 93% of the pixels is corrected

¹ The Cassini VIMS team: K.H. Baines, B.J. Buratti, D.L. Matson, R.M. Nelson, and T.W. Momary at JPL, Pasadena CA, USA; G. Bellucci and V. Formisano at INAF-IFSI, Roma, Italy; F. Capaccioni and P. Cerroni at INAF-IASF, Roma, Italy; R.N. Clark at USGS, Denver CO, USA; D.P. Cruikshank and M.R. Showalter, NASA Ames Research Center, Moffett Field CA, USA; P. Drossart and B. Sicardy at Observatoire de Paris, Meudon, France; R. Jaumann at IPE, Berlin, Germany; CNRS, Nantes, France; N. Baugh and C.A. Griffith at University of Arizona, Tucson AZ, USA; Y. Langevin at IAS, Paris, France; T.B. McCord, G.B. Hansen and C.A. Hibbitts at University of Washington, Seattle WA, USA; V. Mennella at INAF - Osservatorio di Capodimonte, Napoli, Italy; P. D. Nicholson at Cornell University, Ithaca NY, USA; C. Sotin at LPG

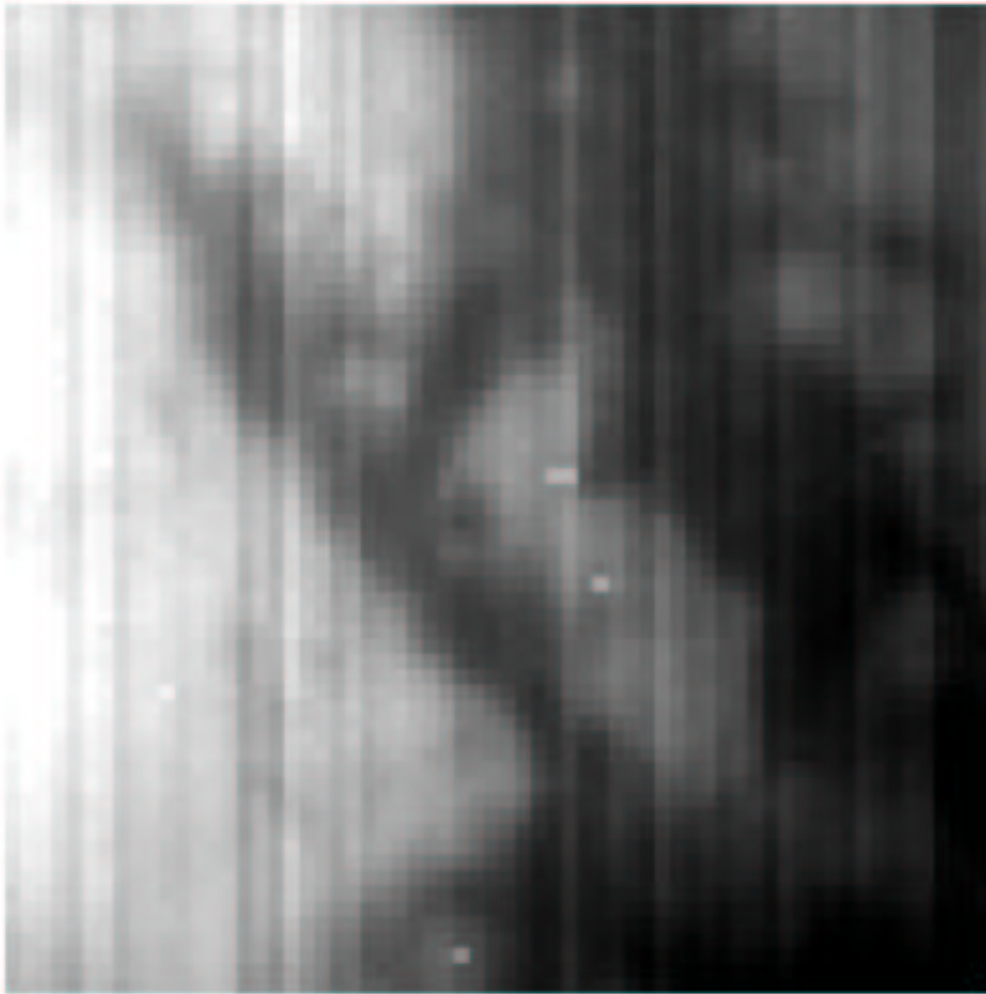


Fig. 1. V1514302573 image relative to the 827.21 nm spectral window.

within the 2% and, finally, the correction results always fall within the 3% of the original values. Some attention has to be paid in applying the destriping procedure to those images showing space background, due to the excess in the pixel intensity's contrast. An improved algorithm has to be developed to overcome this difficulty and this work is now in progress.

3. Minor species observations

After an image archive review, the hyperspectral cube V1526796393, from the S20 Titan flyby, was selected as a case study to identify minor species features in the limb infrared spectrum, both for his good moderate spatial resolution and for his good signal to noise (S/N) ratio. This cube was acquired when the spacecraft was at 91900 km distance from the Titan surface, corresponding to a 45.95×45.95 km for the pixel dimension at Nadir. Easy geometrical calculations,

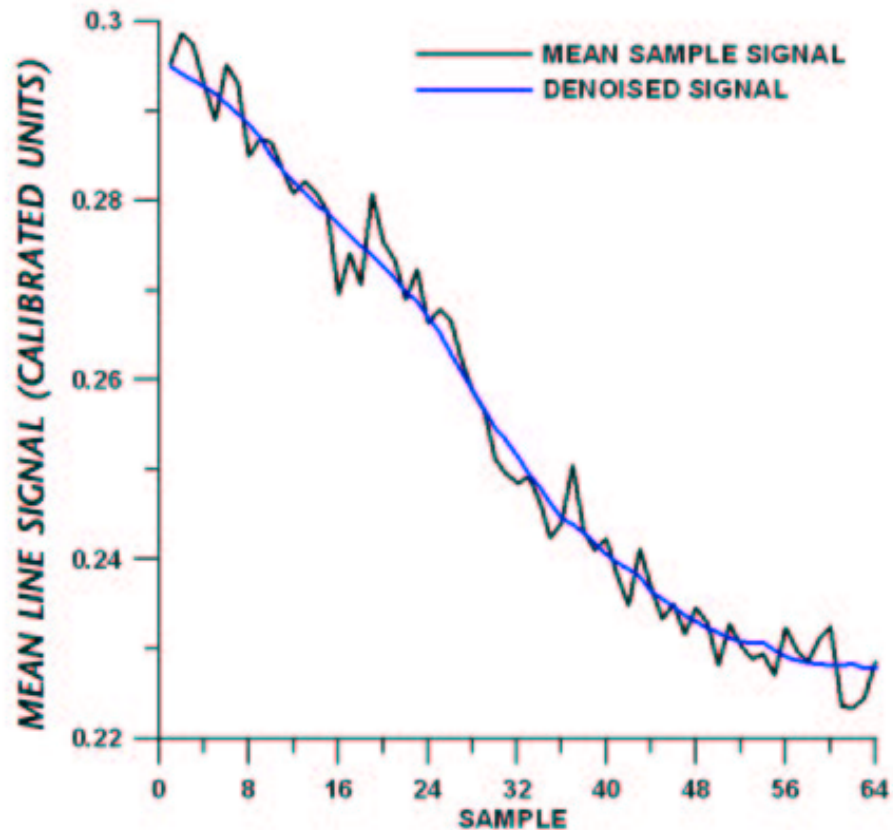


Fig. 2. The mean line signal (black curve) and the denoised sample signal (blue curve) behaviors versus the sample numbers of the Fig. 1 image.

based on the effective IFOV value of the VIMS-IR channel and on Titan radius value, produced an enhanced dimension of 47.2×47.2 km for the limb pixel dimensions. To be sure of considering only atmosphere in the limb spectral analysis, a masking procedure, based on the SPICE geo-referencing calculations and on the ENVI elaboration techniques, has been applied to the RGB image relative to the cube V1526796393, as shown in Fig. 5-6.

Aiming to associate the limb pixel spectra to different heights, starting from the Titan surface, a radial direction, cutting the pixel along their diagonal, has been selected. In this way each pixel spectrum refers to a thickness of ≈ 66.7 km for each layer except the one near the surface that is the half thickness; the radiance contribution to this surface layer can be thought as a mixture of the surface and the lowest atmosphere ones. In Fig. 7 eight VIMS-IR spectra in the range $2.5 - 5.1 \mu\text{m}$, collected along the direction indicated in Fig. 6, are reported, together with the relative estimated heights and the pixel positions.

As it can be seen from the behaviors reported in Fig. 7, the two spectra nearest to the surface are again influenced from the sun radiation reflected by the surface and/or scattered by the

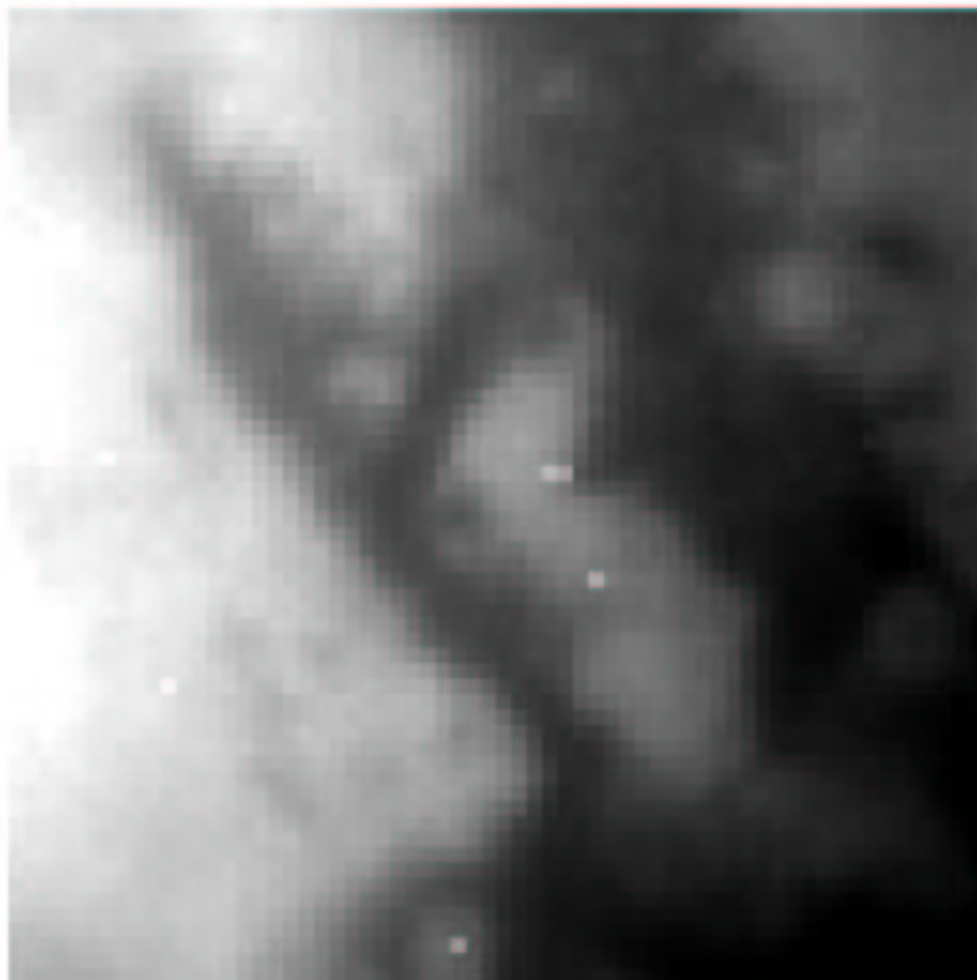


Fig. 3. The same image of Fig. 1 after the destriping procedure.

haze, while, starting from the ≈ 90 km level, the emission features are placed on a quite uniform background. In this article, we intend to highlight the presence of a daytime emission by HCN at $3 \mu\text{m}$; we will discuss moreover other spectral features already reported from other authors for CH_4 (Kim et al. 2000; Brown et al. 2006) at $3.34 \mu\text{m}$ and CO (Baines et al. 2006) from VIMS night-time observation) at $4.76 \mu\text{m}$. The $3 \mu\text{m}$ and the $3.34 \mu\text{m}$ emissions have been identified as C-H stretches of the HCN and $\text{CH}_4 \nu_3$ band respectively (Kim et al. 2000; Geballe et al. 2003; Yelle & Griffith 2003), while different candidates could be responsible for the thermal emission at $4.76 \mu\text{m}$ as can be seen in the Fig. 8, where the absorption intensity spectra by HITRAN 2004 (Rothman L. S. et al. 2004), for some possible molecules inside the Titan's atmosphere, are reported. In Fig. 9 an enhancement of some detailed parts of Fig. 7 are reported.

In the top left panel of Fig. 9 no features are prominent but a general reduction of the reflectance values indicate the decreasing of the surface reflection and haze scattering contribution

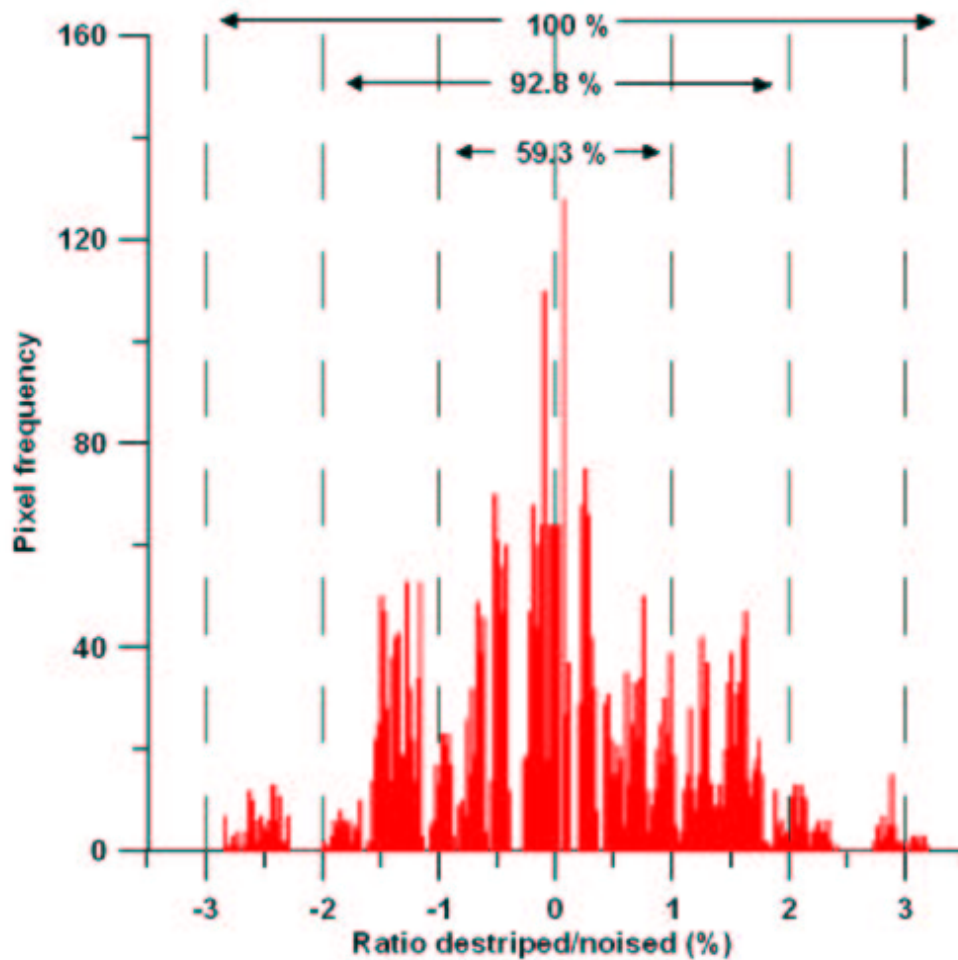


Fig. 4. In this histogram the number of pixel intensities, falling in the 1,2 and 3 σ , are reported. The error (%) class intervals are calculated from the ratio between destriped pixels and \bar{S}_j .

with height increasing. In the top right panel of Fig. 9 the HCN fluorescence is shown: the band maximum difference would indicate a top of concentration corresponding to the 157-224 km layer (violet line), but a strong HCN contribution is evident from the higher layers too. The CH₄ fluorescence is reported in the bottom left panel of Figure reffig:figure9. This result is in good agreement with that one reported in (Brown et al. 2006) for a previous Cassini-VIMS flyby at lower spatial resolution. As can be seen by comparing the top right and bottom left panels the CH₄ fluorescence reflectance is one order bigger than the HCN one and his maximum contribution would seem from the two contiguous 157-224 and 224-290 km layers (violet and blue line). The most relevant thermal emission of the VIMS-IR range is shown in the bottom right panel of Fig. 9. While by the spectral position analysis this feature could be assigned to C₂H₂,

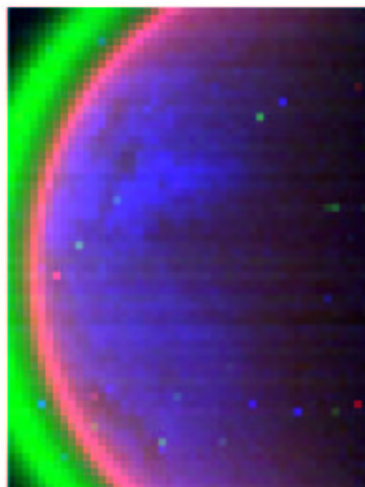


Fig. 5. RGB image of the cube V1526796393_1.QUB_IRCAL, where R=3.032 μm , G=3.333 μm and B=4.77 μm has been selected on the base of the more relevant spectral features in the range 2.5 -5.0 μm .

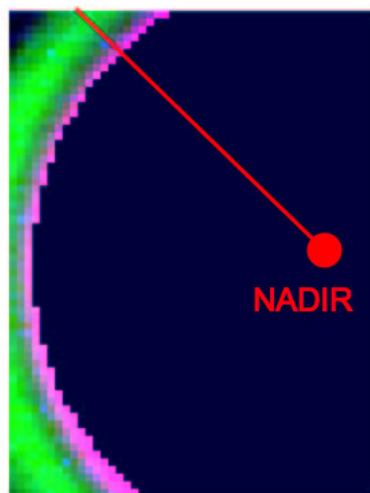


Fig. 6. The same of Fig. 5 after the masking procedure. Also the Nadir position and the direction selected for the pixel spectra collection are indicated in red the image.

HCN, CO_2 and CO, the cross checking between molecular absorption spectra of Fig. 8 and the reflectance spectra of Fig. 7, together with the most qualified photochemical model results, suggest the daytime CO molecule as principal responsible for the 4.76 μm feature. In this last case the contributions seems to be limited to the first layers, with a maximum in the surface layer. In Fig. 10 a visualization of the described results is reported. This visualization has been realized by the band ratio technique (the wavelengths used for the ratios are reported on top of each panel of the figure. This technique applies the differential band method algorithm to the hyperspectral

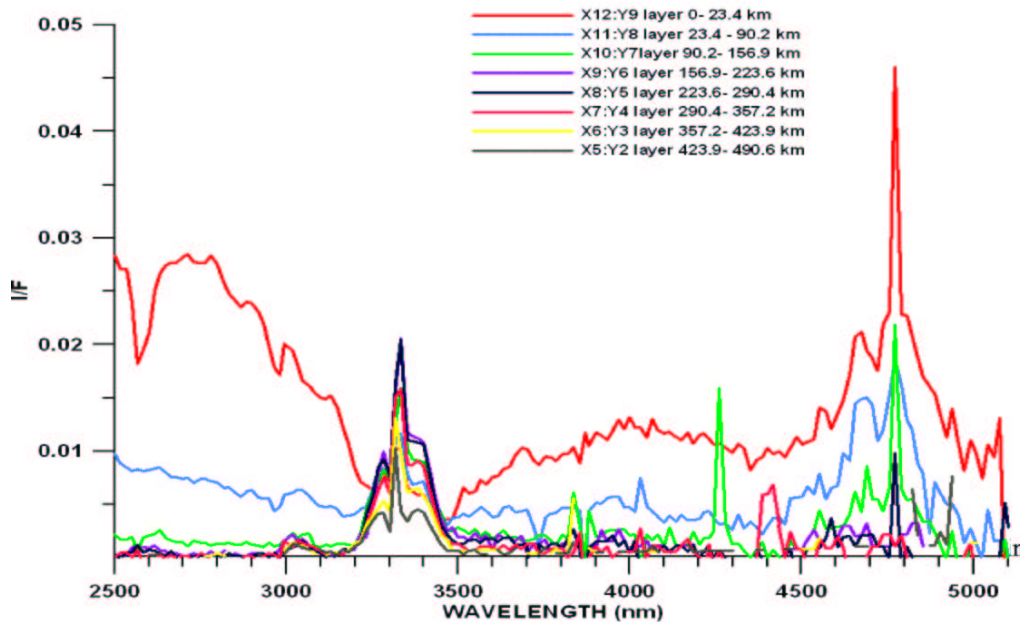


Fig. 7. Spectral reflectance collection for the pixels along the track reported in Figure 6. The wavelength range reported has been selected to enhance HCN and CH₄ fluorescences (Yelle & Griffith 2003; Kim et al. 2000) and other thermal emission features.

images. In the resulting pictures the white in the color scale indicates the maximum intensity value for each pixel ratio and the black the minimum value.

Acknowledgements. This work has been supported by the Italian Space Agency, ASI.

References

- Baines, K. H. et al. 2006, PSS (in press).
 Brown R. H. et al. 2006, AAP, 446, 707
 Geballe T. R. et al. 2003, APJL, 583, 39
 Kim S. J. et al., 2000, Icarus, 147, 588
 Rothman L. S. et al., 2004, HITRAN 2004 Molecular Spectroscopic Database.
 Yelle R. V. & Griffith, C., 2003, Icarus, 166, 107

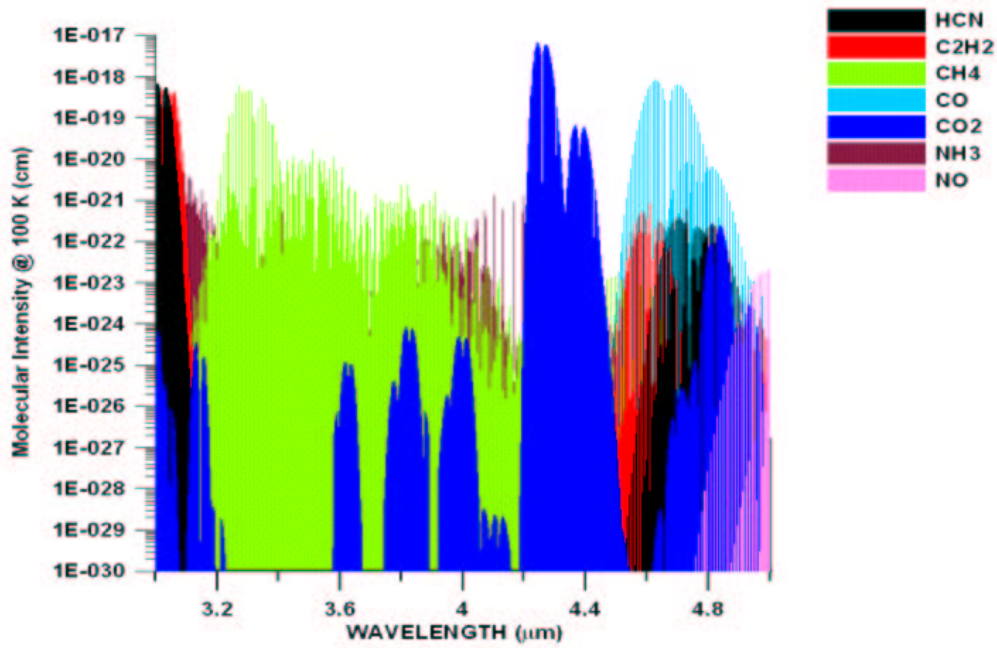


Fig. 8. Absorption intensities of the molecules that could be responsible for the spectral features in the wavelength range 3.0 - 5.0 μm (Rothman L. S. et al. 2004).

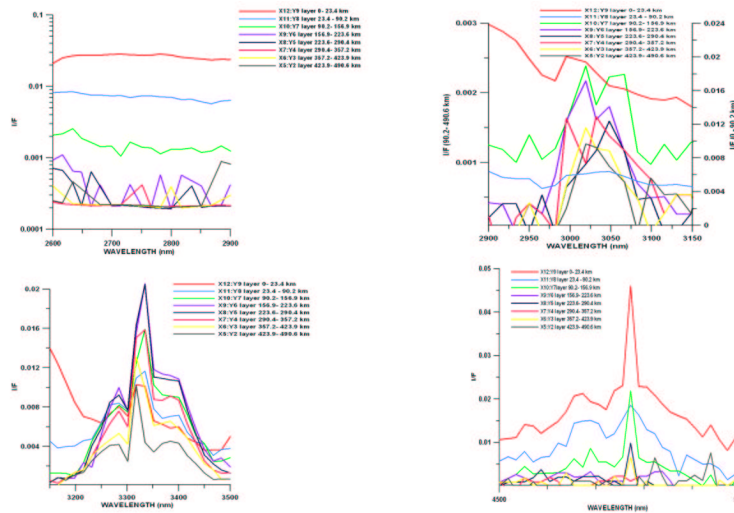


Fig. 9. In the four panels the spectral reflectance of Fig. 7 is reported for the ranges: 2.6 – 2.9 μm (top left panel), 2.9 – 3.15 μm (top right panel), 3.15 – 3.5 μm (bottom left panel) and 4.5 – 5.0 μm (bottom right panel). The enhancement highlights the surface scattering contribution, the HCN and CH_4 fluorescence emissions and a thermal emission assigned principally to a CO contribution.

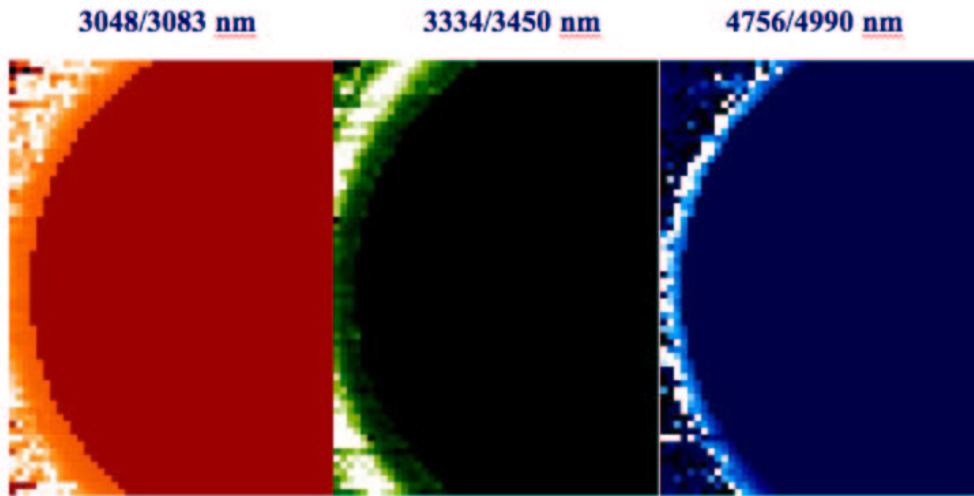


Fig. 10. The three panels have been realized by the band ratio technique (ENVI package). At the top of the pictures the wavelengths used to obtain the image ratio are reported.